DEFINITION OF A SCREENING CRITERION FOR CENTRIFUGAL COMPRESSOR VIBRATIONS INDUCED BY INLET GAS FLOW

Leonardo Baldassarre
Engineering Executive for Compressors and Auxiliary Systems
GE Oil & Gas
Florence, Italy

Michele Fontana
Senior Engineer for Centrifugal Compressors
GE Oil & Gas
Florence, Italy

Andrea Bernocchi
Senior Engineering Manager for Centrifugal Compressors
GE Oil & Gas
Florence, Italy

Alessandro Carnevali
Centrifugal Compressor Design Engineer
GE Oil & Gas
Florence, Italy

Leonardo Baldassarre is currently Engineering Executive Manager for Compressors and Auxiliary Systems with GE Oil & Gas, in Florence, Italy. He is responsible for requisition and standardization activities and for the design of new products for compressors, turboexpanders and auxiliary systems.
Dr. Baldassarre began his career with GE in 1997. He worked as Design Engineer, R&D Team Leader, Product Leader for centrifugal and axial compressors and Requisition Manager for centrifugal compressors.
Dr. Baldassarre received a B.S. degree (Mechanical Engineering, 1993) and Ph.D. degree (Mechanical Engineering / Turbomachinery Fluid Dynamics, 1998) from the University of Florence. He authored or coauthored 20+ technical papers, mostly in the area of fluid dynamic design, rotating stall and rotordynamics. He presently holds five patents.

Andrea Bernocchi is an engineering manager at GE Oil & Gas. He joined GE in 1996 as Centrifugal Compressor Design Engineer after an experience in plastic machinery industry. He has 18 years of experience in design development, production and operation of centrifugal compressor. He covered the role of LNG compressor design manager for 6 years with responsibility in design of LNG compressors, testing and supporting plant startup. He's currently leading the requisition team for centrifugal and axial compressor design.
Mr Bernocchi received a B.S. degree in Mechanical Engineering from University of Florence in 1994. He holds 4 patents in compressor field.

Michele Fontana is currently Engineering Manager for Centrifugal Compressor Upstream, Pipeline and Integrally Geared Applications at GE Oil & Gas, in Florence, Italy. He supervises the calculation activities related to centrifugal compressor design and testing, and has specialized in the areas of rotordynamic design and vibration data analysis.
Mr. Fontana graduated in Mechanical Engineering at University of Genova in 2001. He joined GE in 2004 as Centrifugal Compressor Design Engineer, after an experience as Noise and Vibration Specialist in the automotive sector.
He has co-authored nine technical papers about rotordynamic analysis and vibration monitoring, and holds two patents in this same field.

Alessandro Carnevali is currently Centrifugal Compressor Design Engineer at GE Oil & Gas, in Florence, Italy. His current duties are mainly focused on rotordynamic and thermodynamic design and testing of Centrifugal Compressors for Upstream, Pipeline and Integrally Geared Applications.
He joined GE in 2013 as Centrifugal Compressor Design Engineer, after an experience as thermo-fluid-dynamic engineer in Nuclear Field.
Mr. Carnevali received a Master degree (Energy Engineering) from University of Pisa in 2009.

ABSTRACT

The gas flow entering from the inlet flange of a centrifugal compressor may induce radial forces on the rotor, by directly impinging onto shaft or by generating asymmetric pressure fluctuations in the gas volume surrounding the shaft. This

aerodynamic excitation represents a potential source of radial vibrations for the rotor; it is characterized by a broad-band, low frequency spectrum and its effects are typically observed to increase when the operating point moves towards the top right part of the operating envelope, i.e. at high operating speed and high inlet flowrate.

The severity of the vibrations caused by this airborne excitation depends on the thermodynamic parameters of the inlet gas (flowrate, velocity, density) and on the mechanical design of the compressor (geometry of the suction volume, stiffness of rotor and journal bearings). While the former are generally constrained by process requirements, the latter can be optimized in order to minimize the induced vibrations. Moreover, a very effective way to mitigate this phenomenon is the adoption of Inlet Guide Vanes at compressor suction, that can protect the shaft from exciting forces; on the other hand the installation of IGVs increases the cost and the mechanical complexity of the design, and may also have a non-negligible impact on performances, causing a pressure loss. For this reason it is useful to define a screening criterion to decide whether to install IGVs, based on the predicted sensitivity of the rotor to inlet gas flow excitation. Such criterion was developed basing on physical considerations and then validated through application to a set of recorded references from compressors tested in full load. The outcome allowed to build a diagram based on compressor geometry and operating data, where a boundary line separates the safe area (no significant vibration expected) from the area where the application of IGVs is suggested.

INTRODUCTION

The gas entering from the inlet flange of a centrifugal compressor is a potential source of radial vibrations of the rotor, due to the pressure fluctuations associated to the turbulent flow that create an asymmetric, time-varying pressure distribution around the shaft. These vibrations are characterized by a broad-band spectrum, generally distributed in the frequency range between zero and the synchronous rotating speed, with a maximum amplitude in the central part of this range (often close to the first critical speed of the rotor), as shown in the example of Figure 1. Figure 2 shows the inlet section of a centrifugal compressor, with the nomenclature used in the present work.
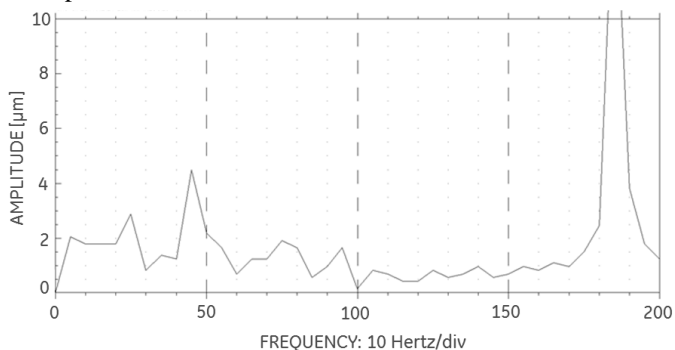

Figure 1. Frequency spectrum of rotor radial vibrations excited by inlet gas flow.
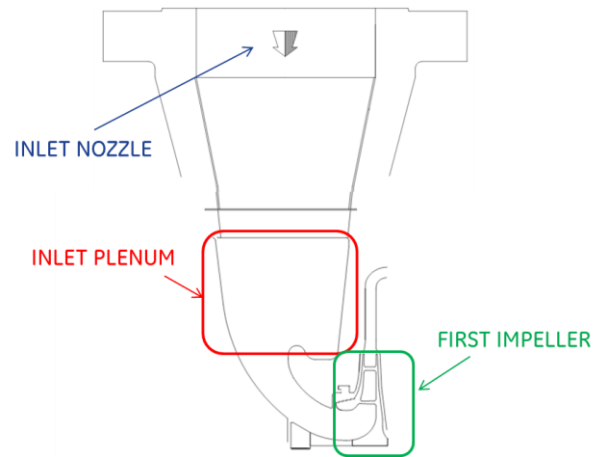

Figure 2. Sectional drawing of a centrifugal compressor inlet portion, from nozzle to first impeller.

This phenomenon is widely discussed in literature for generic physical system such as jet flows impinging on cylinders or plates (Lyon, 1987; Liu and O'Farrell, 1995; De Rosa et al., 2010), but there are very few references to its application to turbomachinery (Jungbauer and Eckhardt, 1997). Rotor vibrations due to inlet gas excitation may be erroneously associated to other rotordynamic phenomena A detailed analysis of the vibration pattern should help to discern the addressed phenomenon from other causes of allows to make a distinction from other causes of subsynchronous vibrations:

- Rotating stall of rotor parts: this phenomenon is usually characterized by subsynchronous vibration typically present in a well defined range. of about 65 to 80 percent of the synchronous frequency (Hagino and Kashiwabara, 2009; Lüdtke, 2004) Moreover, in case of rotating stall the subsynchronous vibration amplitude suddenly decreases when the flow increases, while for inlet gas excitation the amplitude increases with flowrate (see Figure 8 below).

- Rotating stall of stator parts: same considerations of stall rotoric parts are valid; the difference is in the typical range of vibrations measured, which is about 10 to 40 percent of the synchronous one. (Ferrara et al., 2002; Lüdtke, 2004).

- Rotor dynamic instability inception: this phenomenon appears as a narrow-peak sub synchronous vibration close to the first natural frequency of the rotor (Wilcox and O'Brien, 2003; Muszynska, 2005), while vibrations caused by inlet gas excitation usually have a broadband frequency distribution and a maximum amplitude located below the first natural frequency of the rotor.

- Hydrodynamic journal bearing instability: this phenomenon induces a narrow-peak subsynchronous vibration at 40% to 50% of operating speed frequency, that can be altered by varying the lube oil temperature (Bently et al. 1986). Vibration caused by inlet flow excitations are usually not influenced by lube oil parameters and their peak frequency is not proportional to rotating speed.

The present study proposes a formulation based on an analytical model of the phenomenon, to predict the amplitude and the frequency distribution of the pressure fluctuations and

of the consequent rotor vibrations. The formulation is applied to a set of references and compared with experimental data, to validate its predictability; two case studies are presented in detail.

ANALYTICAL MODEL

The broadband aerodynamic force F_a applied by the inlet gas flow on the shaft in the radial direction can be represented by Equation (1), considering a finite number n of frequency intervals between zero and a maximum value, that basing on experience can be assumed as the shaft rotating speed Ω:

$$F_a(t) = \sum F_i \sin(\omega_i t + \alpha_i) \tag{1}$$

considering $\omega_i = 2\pi f_i$, with f_i defined as the center frequency of the ith frequency band. Each value F_i depends on the amplitude of the pressure fluctuations of the gas acting on the shaft, in the corresponding frequency range:

$$F_i = \Delta p_i \cdot A_C \tag{2}$$

where A_C is the planar projection of the rotor surface impinged by the inlet gas flow (see Figure 3). In first approximation it is considered equal to aD, where a is the axial distance between the first point of the rotor in contact with the flowpath and the point of the first spacer where the tangent to its external surface is parallel to the shaft axis, and D is the minimum rotor diameter over a.

According to theory (Lyon, 1987) the magnitude of the pressure fluctuation Δp_i is a function of the frequency and of the total dynamic head p_d. The frequency f is written in adimensional form, using the Strouhal number:

$$St = \frac{fD}{v_r} \tag{3}$$

where $v_r = v \sin\alpha$ is the radial velocity of the gas impinging on the shaft and D is the characteristic length (in this case the rotor diameter at inlet section). The dynamic head is calculated as:

$$p_d = \frac{1}{2}\rho v_r{}^2 \tag{4}$$

where ρ is the gas density at inlet.

In the present model the velocity v of the gas velocity is calculated at section A_R, where the gas flowpath reaches the rotor. Therefore the radial velocity of the gas impinging on the shaft is rewritten as:

$$v_r = \lambda \frac{Q}{A_R} \sin\alpha \tag{5}$$

where Q is the inlet volume flowrate. The adimensional parameter $\lambda \geq 1$, named *inlet velocity distribution factor*, is introduced to quantify the circumferential uniformity of the gas velocity. It is defined as the ratio between the maximum and the average gas velocity over A_R. $\lambda = 1$ represents the ideal case

of a perfectly uniform velocity distribution, while for actual inlet geometries the gas velocity is usually higher in the part closer to the inlet flange location.
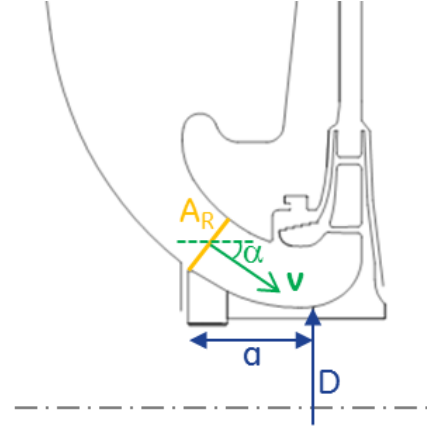

Figure 3. Inlet gas velocity and geometric parameters of compressor inlet portion.

For an impinging flow the relation between the overall peak-to-peak amplitude of the pressure fluctuation Δp_{OA} and the dynamic head p_d is approximated by Equation (6), and the relation between Δp_i and Δp_{OA} is given by the adimensional curve $g(St)$ shown in Figure 4 (Lyon, 1987).

$$\Delta p_{OA} = 0.084 p_d = 0.042\rho \left(\lambda \frac{Q}{A_R} \sin\alpha\right)^2 \tag{6}$$

The curve $g(St)$ is constant for every rotor. It does not depend on gas conditions, rotor geometry or any other operating parameters:
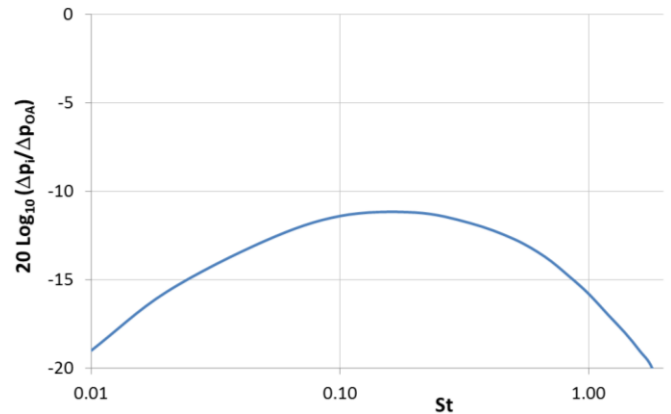
$$\Delta p_i = \Delta p_{OA} \cdot g(St) \tag{7}$$

Figure 4. The curve g(St) represents the relative amplitude of the pressure fluctuations in function of their adimensional frequency. This spectrum is in third-octave band.

The spectral analysis of turbomachinery vibration is usually performed over equally spaced frequency intervals (constant bandwidth) rather than in octave or third-octave frequency bands, and amplitude values are expressed in linear scale rather than in dB scale. For this reason the curve $g(St)$ is represented

in a more convenient form in Figure 5. Numbers on the vertical axis of that diagram are not shown because the amplitude of the curve depends on the frequency resolution considered for the spectrum, even if its shape remains unchanged.
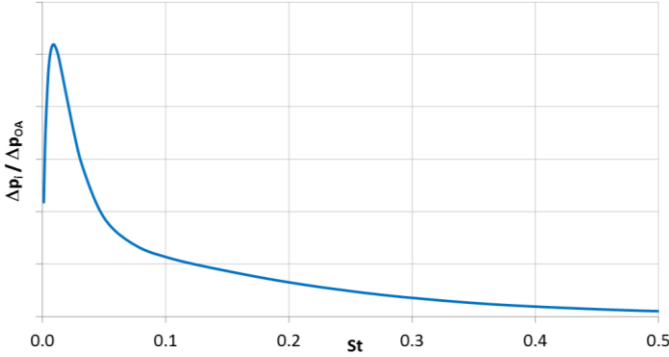

Figure 5. Same curve g(St) of Figure 4, plotted as equally-spaced frequency spectrum on linear vertical scale.

Combining Equations (2) and (6) by means of the above relation (7) and remembering that $A_C=aD$, the force component F_i is rewritten as:

$$F_i = 0.042 a D \rho \left(\lambda \frac{Q}{A_R} sin\alpha \right)^2 g(St) \qquad (8)$$

The amplitude x_i of the displacement caused by the sinusoidal force component F_i is here assumed as proportional to the exciting force and inversely proportional to the radial stiffness k (Hooke's law):

$$x_i = \frac{F_i}{k} \qquad (9)$$

k is the equivalent dynamic stiffness of the system (rotor plus journal bearings), whose amplitude can be written as:

$$k = \sqrt{\left(k_{eq} - M\omega^2\right)^2 + (c\omega^2)^2} \qquad (10)$$

where the equivalent stiffness k_{eq} results from the radial stiffness of the two journal bearings acting in parallel, combined with the bending stiffness of the rotor journal bearing stiffness (see sketch in Figure 6) and M is the rotor mass. The trend of k as function of frequency is exemplified in Figure 7: it has a maximum in correspondence of the critical speed ω_0 of the system.
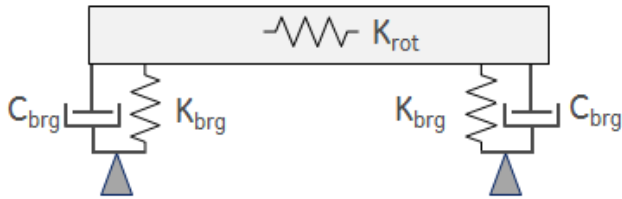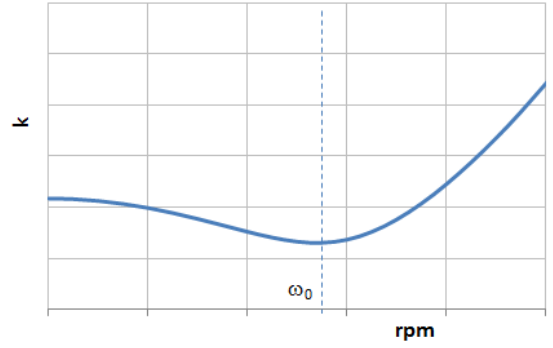

Figure 6. Rotor plus journal bearing system.

Figure 7. Example plot of radial stiffness vs. frequency.

Combining Equations (8), (9) and (10) the displacement amplitude x_i is written as:

$$x_i = \frac{0.042 a D \rho \left(\lambda \frac{Q}{A_R} sin\alpha \right)^2 g(St)}{\sqrt{\left(k_{eq} - M\omega_i^2\right)^2 + (c\omega_i^2)^2}} \qquad (11)$$

When applying this calculation model as a predictive tool for rotordynamic assessment, its outcome shall be compared with a conveniently set acceptance limit. The limit can be imposed on the maximum amplitude of each component x_i, in line with the API approach that imposes a limit on nonsynchronous vibration amplitude (API617, 2014).

The formulation of Equation (11) clearly shows all the main parameters that have an influence on rotor vibrations caused by inlet gas flow. For some process or geometric parameters (ρ, Q, M, D) variations may have big impact on the design or be not possible at all, and the journal bearing charachteristics (k, c) are usually already optimized. Variations of a, A_R and α can be considered but are limited by aerodynamic and rotordynamics constraints, and may also have a negative impact on compressor performance. The main focus shall then be put on improving the uniformity of the inlet gas velocity, to reduce the value of λ. This can be achieved by optimizing the design of the inlet plenum and most effectively by applying IGVs to the inlet section.

Finally it shall be noted that any calculated or imposed value of x_i shall always be referred to a value of frequency spectrum resolution. In fact the amplitude of overall vibrations and of pure tones (single-frequency peaks) does not depend on spectral resolution, while the peak amplitude of any distributed (broadband) signal such as $g(St)$ can be influenced by it.

MODEL VALIDATION FROM EXPERIMENTAL DATA

The analytical model described above was applied to a set of 29 centrifugal compressors manufactured and tested at full load by authors' company in the past fifteen years. Vibration spectrum components associated to inlet gas excitation were detected on a subset of 8 compressors, and were significantly high on 3 of them that are here presented as case studies (see Table 1). These machines cover different design types: Unit #1 is a large compressor with horizontally-split casing, Unit #2 is a pipeline compressor with barrel casing and nozzles on opposite sides and Unit #3 is a high pressure barrel compressor with

nozzles on the same side. All the units consist of a single compression section with in-line stage arrangement.

Unit	No. stages	Gas density at inlet [kg/m^3]	Rotor Mass [kg]	Shaft Diameter [m]	CS1 [cpm]
#1	2	18.2	2250	0.29	3500
#2	2	52.2	1030	0.205	3380
#3	6	121.4	300	0.150	5840

Table 1. Centrifugal compressors considered as case studies.

Unit #1 was one of the first compressors where subsynchronous vibration related to gas inlet excitation were observed during the test. A specific test was carried out to analyze the relationship between gas flow and vibration amplitude. The peak amplitude of subsynchronous vibration was recorded over a range of inlet flowrate, keeping constant inlet gas pressure, temperature and composition. The results are plotted in Figure 8.
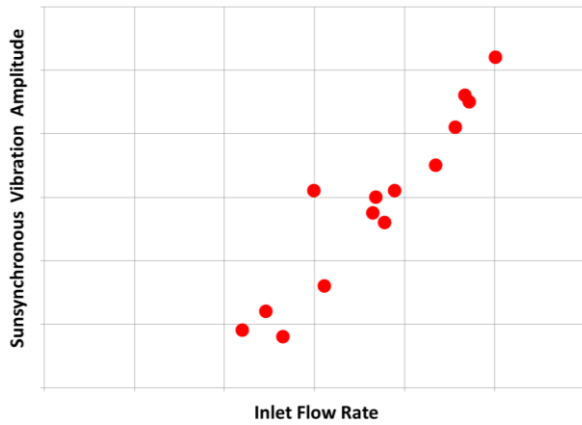

Figure 8. Subsynchronous vibration vs gas inlet flowrate measured on Unit #1.

The results show a strong relation between flowrate and vibration amplitude, as predicted by Equation (11).

Unit# 2 is a pipeline compressor manufactured in the late 90's. During the full load test at maximum continuous speed (MCS) high subsynchronous vibrations were recorded, as reported in the frequency spectrum of Figure 9.
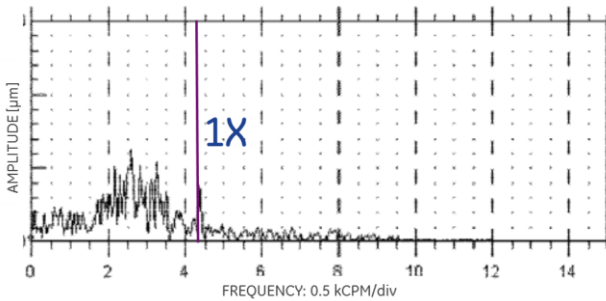

Figure 9. Subsynchronous vibration measured during the test of Unit #2.

A test similar to the one performed for Unit #1 was also carried out for Unit #2 (see Figure 10), showing a qualitatively similar correlation between the inlet flowrate and the subsynchronous vibration.
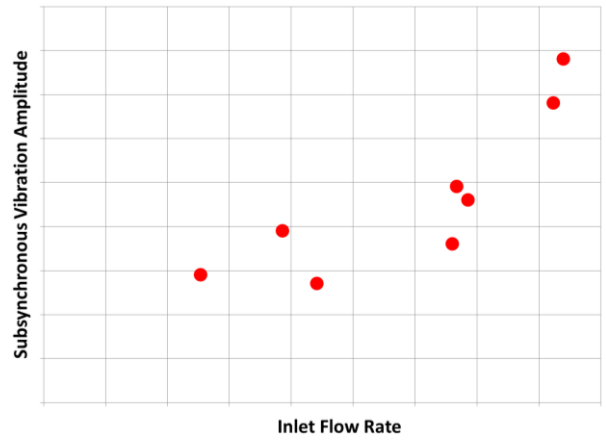

Figure 10. Subsynchronous vibration amplitude vs inlet volume flow for Unit #2.

Unit#3 is a high pressure barrel compressor. During the test, a broad-band, low frequency spectrum was recorded as reported in Figure 11. Relatively high subsynchronous vibrations were measured.
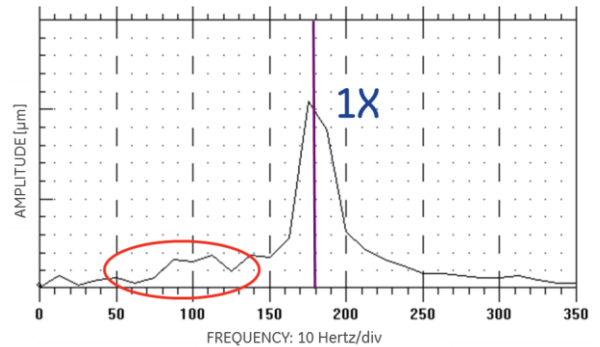

Figure 11. Subsynchronous vibration measured during the test of Unit #3.

The waterfall plots recorded during the startup and shutdown test of Unit #3 are plotted in Figures 12-13, to highlight the features of the subsynchronous vibration: broadband, non-periodic (peaks are not exactly at same frequencies for each spectrum) and higher at higher inlet flow rate, i.e. at higher speed during the startup/shutdown transients.
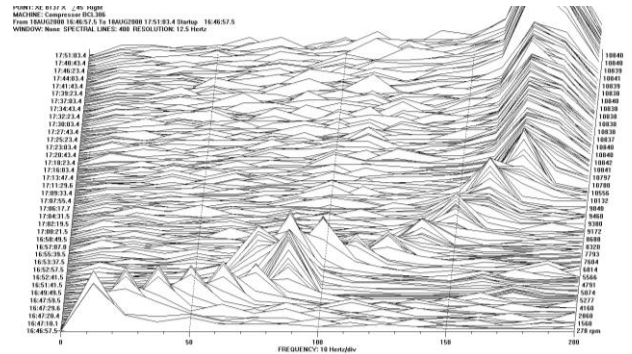

Figure 12. Waterfall plot of Unit #3 during start up.
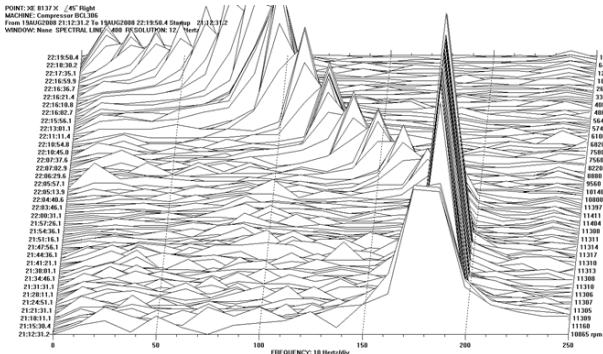
Figure 13. Waterfall plot of Unit #3 during coast down.

The vibration amplitude due to inlet gas excitation was calculated for all the reference compressors by applying the analytical model described in this work. The results sre reported in detail (plot of vibrations amplitude vs. frequency) for the three case studies in Figure 14, and in summary for all the 29 references in Figure 15, ordered from left to right by predicted peak amplitude of the subsynchronous vibration.

Figure 14 shows similar trends, characterized by a peak at low frequency and by high peak amplitude compared to compressors that did not show subsynchronous vibrations during the load test; one of them (labeled Unit #4) is reported as example. Figure 15 shows the peak vibration amplitude calaulcted for each reference compressor; red bars identify the 8 units where subsynchronous vibration was detected during the test, while green bars represent the compressor that did not show such vibration. The results of the calculation model show a good degree of accuracy in separating the 8 units that actually showed subsynchronus vibrations from the rest of the reference set. A threshold value (blue line on the diagram) can be defined, to be used as acceptance limit during the design phase of new projects. The design of compressors falling above this threshold can be optimized as discussed in the next section.
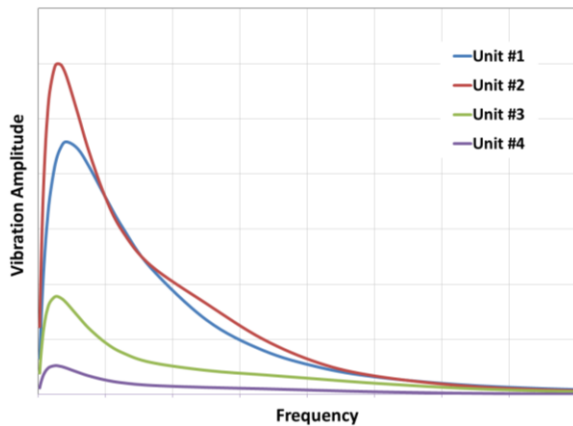

Figure 14. Vibration amplitude calculated for the 3 case studies, and for a compressor that did not show subsybchronous vibration.

MITIGATION OF SUBSYNCHRONOUS VIBRATION RISK

As highlighted by Equation (11), the key parameters that influence the subsynchronous vibration amplitude are the gas properties at inlet, the stiffness and damping coefficients of the system and the geometry of the inlet section of the compressor. Most of these parameters are often unpractical to change, and for some of them variations may be prevented due to contract requirements; the exception is the inlet velocity distribution factor λ, that can undergo significant variations as consequence of relatively small changes of the compressor geometry.
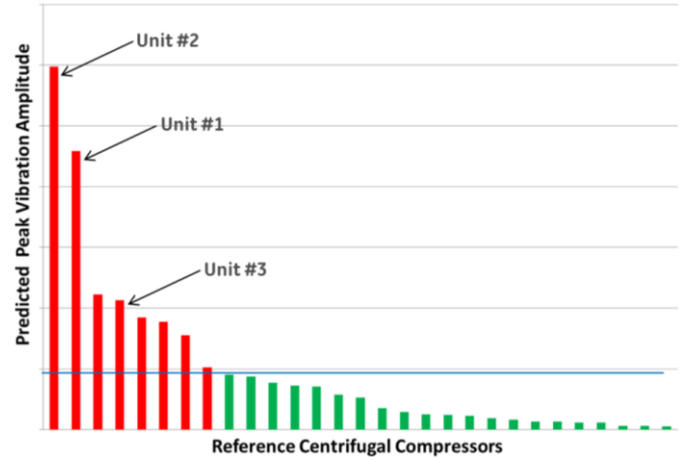

Figure 15. Predicted subsynchronous vibration amplitude for a set of reference compressors.

$$\lambda = \frac{v_{r\_max}}{v_{r\_avg}} \tag{12}$$

where v_{max} is the highest value of the gas velocity at section A_R, at any angular position around the rotor axis (usually at the same angular position of the inlet nozzle axis) and v_{avg} is the average value over the whole circumference. According to CFD results, for a non-optimized inlet geometry the value of λ typically ranges between 2 and 2.5. Lower values (roughly down to 1.5) can be obtained with optimized geometries, such as in the example of Figure 2: large, variable-section inlet plenum and smooth transition between plenum and first impeller, with large curvature radii and uniform reduction rate of the passage area. A further reduction of λ, down to 1.1 or even less, can be reached with the introduction of inlet guide vanes. The value λ shall be estimated by means of a dedicated CFD analysis on the proposed inlet geometry, or interpolated by comparison with similar geometries.

Optimization of inlet plenum

A first method to get a more homogeneous velocity field around the shaft and therefore to reduce the value λ is to optimize the inlet plenum geometry. Figure 16 shows a comparison between the CFD results obtained for four different inlet plenum designs on a large, low-pressure centrifugal compressor with horizontally split casing. The analysis was carried out considering the same gas inlet conditions for all the cases.

As can be seen by comparing Figures 16 and 17, even limited changes to the geometry of the inlet plenum may have a strong impact on the velocity field distribution. In this example the value of λ factor ranges between 1.4 and 1.8.
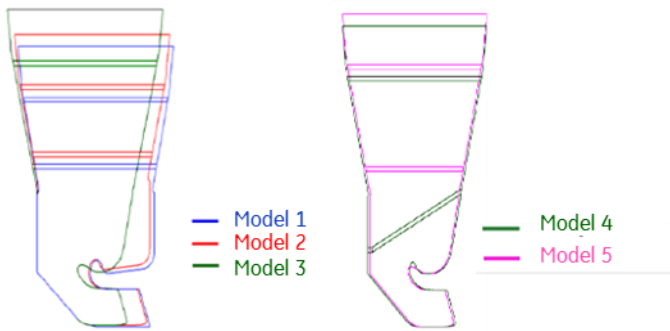
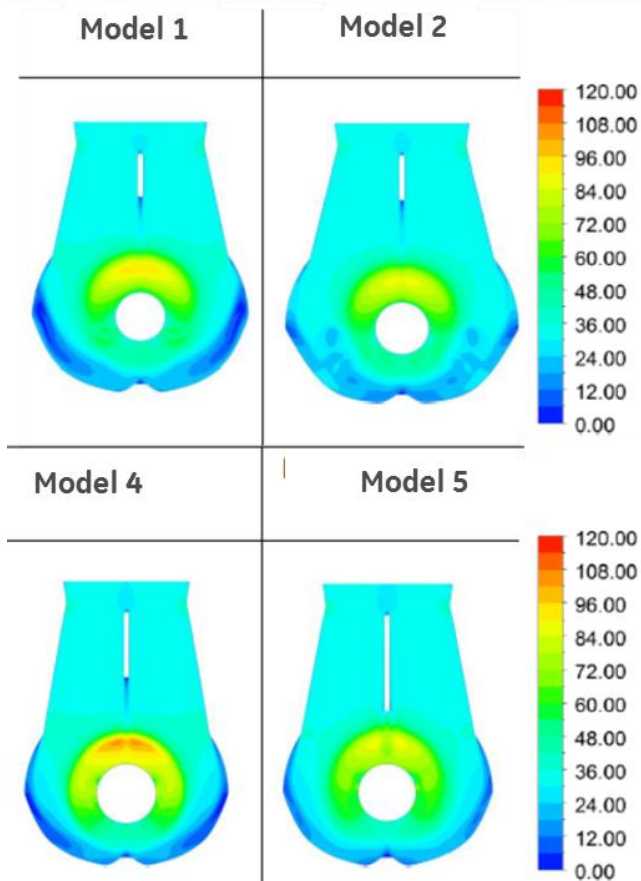*Figure 16. Different inlet plenum geometries evaluated by CFD.*

Figure 17. CFD analyses results for velocity contours on the mid-section.

Inlet Guide Vanes

The installation of IGV (located on the shaft just before the first impeller; generally with fixed geometry, as shown in Figure 18) is another way to improve the uniformity of the gas velocity at inlet.

Several CFD analyses were carried out to investigate the impact of IGV installation on the velocity field distribution. The results presented in Figure 19 refer to a calculation performed on the inlet plenum of a barrel compressor, with and without IGV, for the same plenum geometry and inlet gas
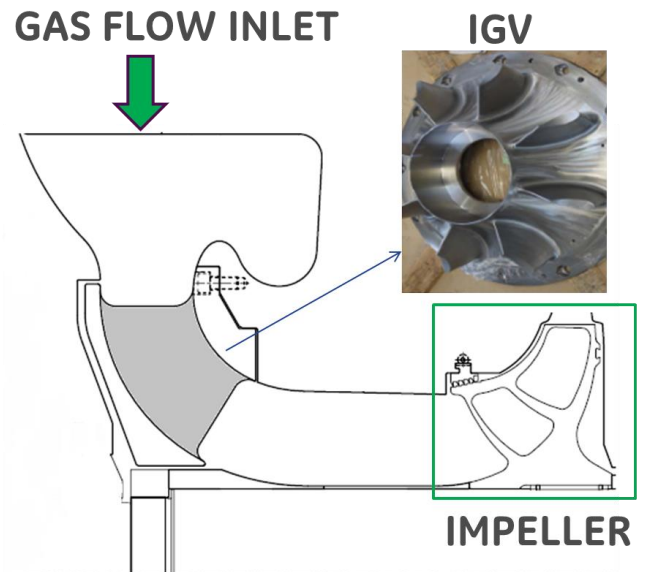
conditions.
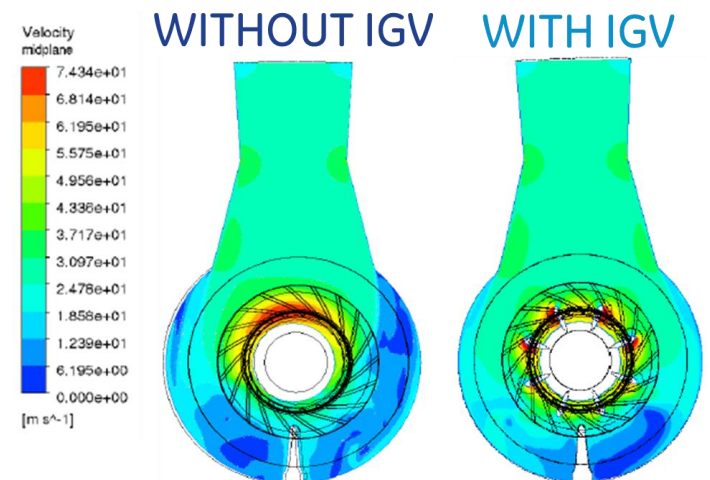

Figure 18. Typical arrangement of fixed-geometry IGVs.

Figure 19. CFD analyses results for velocity contours on the mid-section.

With IGV installed, the velocity field around the shaft was homogeneous (λ almost equal to 1), while without IGV there is a non-uniform distribution leading to λ approximately equal to 2.1.

The positive effect predicted by CFD for the IGV installation was validated by the results of a dedicated test made on Unit #1. Figure 20 shows the average subsynchronous vibration measured during the full load test at different flowrates, before IGV installation (red dots, same of Figure 8) and after (green squares). As it can be seen, the impact is strong, especially at high flow rate.

From a design perspective it shall be noted that while the optimization of the inlet plenum is always positive for compressor efficiency (reducing the pressure losses in the inlet section) and has no impact on costs, the installation of IGVs represents an additional cost and increases the mechanical complexity of the design, and moreover can have a negative

impact on compressor efficiency, particularly at high flowrate where the presence of IGV causes additional pressure losses. Below is a comparison between the polytrophic efficiency measured on a pipeline compressor (Unit #2) with and without IGV. At high flowrate the efficiency is higher when IGVs are not installed.
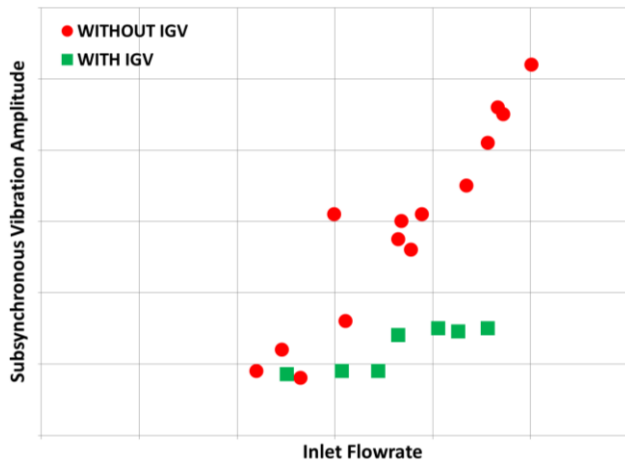

Figure 20. Unit #1 average vibration amplitude vs. flowrate before and after IGV installation.

In summary the installation of IGVs is an effective way to mitigate the risk of rotor vibrations due to inlet flow, but it has some drawbacks; for this reason it is useful to develop an analytical criterion to evaluate the criticality of a compressor design, and to define a threshold limit for IGV application.
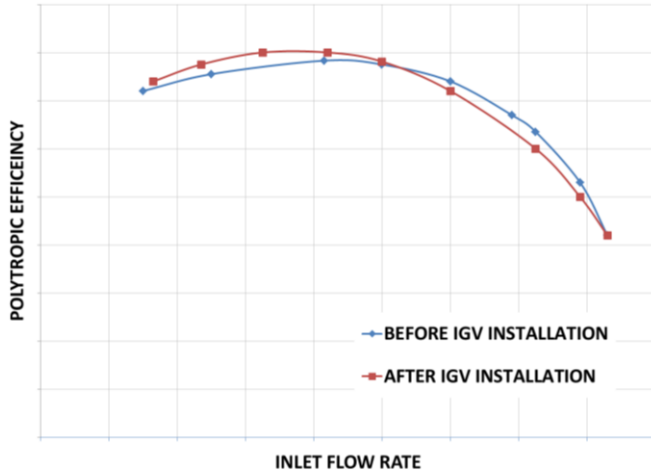

Figure 21. Measured polytropic efficiency vs flowrate for Unit #2, with and without IGV.

DEFINITION OF A SCREENING CRITERION FOR IGV APPLICATION

The analytical model presented in this paper and summarized by Equation (11) was used to develop a criterion for IGV installation. Neglecting the parameters that have smaller effect on vibration amplitude or whose variation is limited to a relatively small range, the rotor sensitivity to vibrations induced by inlet flow can be represented by the diagram of Figure 22. The diagram was populated with a

reference set of existing compressors, that allowed to define a threshold limit between the areas where IGV installation is recommended or not. The compressors where subsynchronous vibrations due to inlet gas excitation were detected are plotted in red, while the ones with no significant subsynchronous was recorded are in green.

The user is required to input only few geometry and process parameters, that should be readily available once the preliminary compressor design is defined:
- Journal bearing damping coefficient c, evaluated at minimum clearance and at 1st critical speed
- First critical speed ω
- F, aerodynamic force of the gas calculated as

$$ F = aD\rho \left(\frac{Q}{A_R} sin\alpha \right)^2 \tag{13} $$

with:
- D, shaft diameter
- a, characteristic length of the shaft impinged by gas
- ρ, gas density at compressor inlet
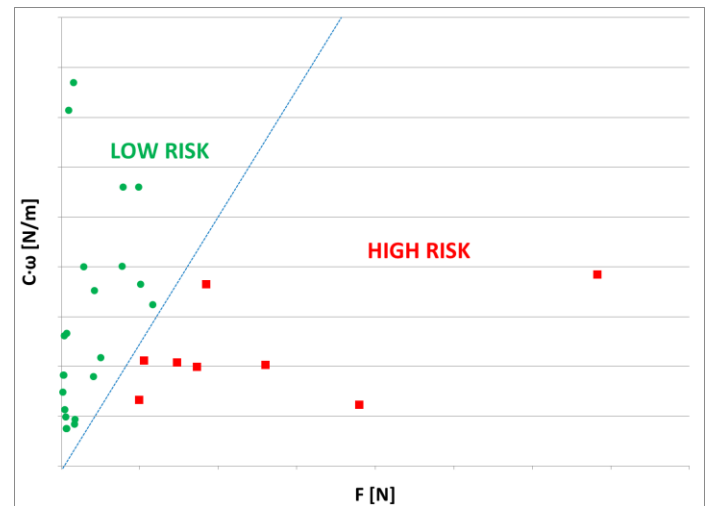- $(Q/A_R)sin\alpha$, gas velocity.

Figure 22. Screening diagram to be used to evaluate the risk of sub-synchronous rotor vibrations due to inlet gas excitation.

CONCLUSIONS

The phenomenon of subsynchronous vibrations on the rotor due to the inlet gas flow impinging the shaft was investigated both from a theoretical and an experimental standpoint. An analytical model of the vibration mechanism was developed and then validated by application to an extensive set of centrifugal compressors tested at full load, including several units that where such subsynchronous vibration was detected during the test. The results highlighted a strong agreement between model predictions and test outcome.

The main parameters influencing the amplitude of subsynchronous vibration were identified and discussed; in particular the Inlet Velocity Distribution Factor (λ) was introduced, highlighting the relation between its value and the geometry of inlet section of the compressor. This included general guidelines to optimize the inlet section design, and to

install Inlet Guide Vanes when necessary.

Based on the analytical model, a simple screening criterion valid for all types of centrifugal compressors was developed, to assess the potential risk of high subsynchronous vibrations and the consequent need for IGV installation. Knowing the values of few geometry and operating parameters, a compressor design can be represented on a sensitivity diagram where a threshold curve separates the high and low sensitivity zones, and compared to a set of references.

NOMENCLATURE

IGV   Inlet Guide Vanes
MCS   Maximum Continuous Speed
OA   Overall
St   Strouhal Number

a Axial Distance [m]
A Section [m^2]
c Damping coefficient [Ns/m]
D Diameter [mm]
F Force [N]
f Frequency [Hz]
g Scalar function [-]
k Stiffness coefficient [N/m]
M Mass [kg]
p Pressure [bar]
Q Volume flowrate [m^3/s]
t Time [s]
v Gas velocity [m/s]
x displacement [m]
α Phase angle [°]
λ Inlet Velocity Distribution Factor [-]
ρ Gas density [kg/m^3]
ω Angular velocity [rad/s]
Ω Shaft rotating speed [rpm]

REFERENCES

API 617, Ch.2, para. 6.3.1.2.2., 2014, "Axial and Centrifugal Compressors and Expander-Compressors for Petroleum, Chemical and Gas Industry Services", Eighth Edition, American Petroleum Institute, Washington, D.C.

Bently, D., Zimmer, S., Palmetier, G. and Muszynska, A., 1986, "Interpreting Vibration Information from Rotating Machinery." *Sound and Vibration magazine*. Volume 20, No. 2. pp. 14-23.

De Rosa S., Franco F. and Gaudino D., 2010, "Low frequency range response of a plate to different turbulent boundary layer excitation models", *Proceedings of ISMA 2010*, Leuven, Belgium, pp. 625-638.

Ferrara, G., Ferrari, L. and Baldassarre, L., 2002, "Rotating Stall in Centrifugal Compressor Vaneless Diffuser: Experimental Analysis of Geometrical Parameters Influence on Phenomenon Evolution", *International Journal of Rotating Machinery,* Hindawi Publishing Corporation, New York, NY, pp.433-442.

Hagino, N. and Kashiwabara, Y., 2009, "Experimental Study of Surge and Rotating Stall Occurring in Small Centrifugal Compressor", *Proceedings of the 45th AIAA/ASME/SAE/ASEE Joint Propulsion Conference & Exhibit*, Denver, CO.

Jungbauer, D. and Eckhardt, L., 1997, "*Flow-induced turbocompressor and piping noise and vibration problems-identification, diagnosis, and solution*, Proceedings of the 26th Turbomachinery Symposium, Turbomachinery Laboratory, Texas A&M University College Station, Texas, pp. 79-85.

Liu, B.-L. and O'Farrell, J.M., 1995, "High Frequency Flow/Structural Interaction in Dense Subsonic Fluids", NASA, Marshall Space Flight Center, AL.

Lyon, R.H., 1987, "Machinery Noise and Diagnostics", Butterworth Publishers, Stoneham, MA.

Lüdtke, K.H., 2004, "Process Centrifugal Compressors", Springer-Verlag, Berlin, Germany.

Muszynska, A., 2005, "Rotordynamics", CRC Press, Boca Raton, FL.

Wilcox, E. and O'Brien, D., 2003, "Determining the Root Causes of Subsynchronous Instability Problems in Two Centrifugal Compressors", *Proceedings of the 32th Turbomachinery Symposium*, Turbomachinery Laboratory, Texas A&M University College Station, Texas, pp. 9-20.

ACKNOWLEDGEMENTS